AUT Journal of Electrical Engineering

AUT J. Electr. Eng., 56(3) (2024) 389-398
DOI: 10.22060/eej.2024.22949.5577

Comprehensive Study on Optical, Electrical, and Stability Properties of $BA_2PbBr_{4-x}Cl_x$ (x = 0, 2, and 4) Ruddlesden Popper Perovskites for High-Performance PeLEDs

Samad Shokouhi[1], Seyedeh Bita Saadatmand[1], Vahid Ahmadi[2,*], Farzaneh Arabpour Roghabadi[1]

[1] Faculty of Electrical and Computer Engineering, Tarbiat Modares University, Tehran, Iran
[2] Faculty of Chemical Engineering, Tarbiat Modares University, Tehran, Iran

ABSTRACT: Two-dimensional (2D) perovskites in the Ruddlesden Popper (RP) structure are commonly employed in optoelectronic applications. This research introduces $BA_2PbBr_{4-x}Cl_x$ (x=0, 2, and 4) as a mixed-halide 2D perovskite material for use in the active layer of perovskite light-emitting diodes (PeLEDs). By utilizing density functional theory (DFT), the electrical, optical, and stability properties of $BA_2PbBr_{4-x}Cl_x$, which have not been previously reported, are investigated. The results show that with an increasing value of x, the bandgap energy shifts towards higher energies (blue shift), while the refractive index decreases. In addition, we demonstrate the band-edge orbitals by analyzing the partial density of states (PDOS) and observing the effect of halide change on them. In the case of x=0 (BA_2PbBr_4), the thermodynamic stability is lower compared to the other two states: $BA_2PbBr_4Cl_2$ (x=2) and BA_2PbCl_4 (x=4). The thermal stability of these materials is studied using the ab initio molecular dynamic (AIMD) method. Furthermore, the stability of these materials in relation to water is also investigated, aligning with the results of thermodynamic stability. The research also explores the influence of strain on bandgap and refractive index. The results show that all three materials are thermodynamically stable, with direct and large band gaps suitable for blue PeLED applications.

Review History:
Received: Jan. 28, 2024
Revised: May, 05, 2024
Accepted: May, 13, 2024
Available Online: Jul. 01, 2024

Keywords:
Density Functional Theory
Mixed-halide 2D-Perovskites
Band Structure
Thermodynamical Stability
Moisture Stability

1- Introduction

In recent times, the expanded utilization of perovskite semiconductor materials has been driven by their fascinating electrical, optical, and mechanical characteristics. These materials have found extensive applications in various optoelectronic devices, including LEDs, lasers, solar cells, and sensors [1-4]. The Ruddlesden-Popper (RP) quasi-two-dimensional perovskite materials can be described by the general chemical formula $(L)_2(A)_{n-1}BX_{3n+1}$ (where n is an integer), wherein L, A, B, and X represent the spacer cation, small cation, metal cation, and anion, respectively. When n=1, the quasi-2D perovskites take on a two-dimensional structure, while for n=∞, they exhibit similarities to three-dimensional (3D) perovskites. Notably, 2D perovskites boast enhanced environmental and thermodynamic stability when compared to their 3D counterparts. Their structure bears resemblance to a multi-quantum well (MQW), featuring the spacer cation (L) as a quantum barrier and the inorganic layer (BX_4) as the quantum well [5].

To create a white perovskite light-emitting diode (PeLED), it is imperative to improve the efficiency of the blue PeLED. Two significant approaches to achieving a highly efficient blue PeLED involve the utilization of 2D-perovskite and mixed-halide materials [6]. Among the experimental candidates, the material $BA_2PbBr_{4-x}Cl_x$ (with x values of 0, 2, and 4) is commonly employed to fabricate blue PeLED [7].

Previous studies have examined the electronic and optical properties as well as the thermodynamic stability of the BA_2PbI_4 material using density functional theory (DFT) [8, 9]. However, for the $BA_2PbBr_{4-x}Cl_x$ (with x values of 0, 2, and 4), it is necessary to assess all the characteristics and stability.

In this study, we employ DFT to analyze the electrical and optical properties, as well as the moisture stability and thermodynamic stability of the $BA_2PbBr_{4-x}Cl_x$ (with x values of 0, 2, and 4) structure. The thermal stability of the materials is also assessed using the ab initio molecular dynamic (AIMD) method. In addition, the study investigates the impact of strain (compression and tensile) on the bandgap (E_g) and refractive index (RI) values. This examination aims to evaluate its suitability for blue PeLED applications. Our findings indicate that BA_2PbCl_4 exhibits thermodynamic stability, and substituting chlorine for bromine leads to an increased bandgap value.

2- Theory

2- 1- Electrical and optical properties

DFT calculations are carried out in the CASTEP module utilizing the Kohn-Sham equation. The equation is defined as follows:

*Corresponding author's email: v_ahmadi@modares.ac.ir

Table 1. Crystal data for the proposed 2D-perovskites

Materials of 2D-perovskite	Crystal structure	Lattice parameters (Å)
BA_2PbBr_4	Orthorhombic	a=8.33, b=8.21, c=27.58, α=β=γ=90°
$BA_2PbBr_2Cl_2$	Orthorhombic	a=8.15, b=8.02, c=27.79, α=β=γ=90°
BA_2PbCl_4	Orthorhombic	a=7.98, b=7.86, c=27.97, α=β=γ=90°

$$[T+U]\phi_i(r)=\varepsilon_i\ \phi_i(r)$$
$$T=-\nabla^2/2, U=V_n(r)+V_H(r)+V_x(r)+V_c(r) \quad (1)$$

where T represents the kinetic energy and U is the potential energy. U comprises the nuclear potential ($V_n(r)$), Hartree potential ($V_H(r)$), exchange potential ($V_x(r)$), and correlation potential ($V_c(r)$). Additionally, $\phi_i(r)$ and ε_i denote the Kohn-Sham wavefunctions and eigenvalues, respectively [10]. The Kohn-Sham equation is solved by the software with the iterative self-consistent field (SCF) method. From the results, the eigenfunctions, eigenvalues, electron density, total energy, and the parameters required to obtain the various properties including the stability of the material are calculated.

By utilizing the eigenvalues derived from the Kohn-Sham equation, various electronic properties including the band structure, band gap, and partial density of states (PDOS) can be determined. The computation of the imaginary part of the complex dielectric function ($\varepsilon_2(\omega)$) can be achieved as described in [11]:

$$\varepsilon_2(\omega)=\frac{2q^2\pi}{V\varepsilon_0}\sum_{k,v,c}\left|<\psi_k^c|\,p.r\,|\psi_k^v>\right|^2\delta\left(E_k^c-E_k^v-\hbar\omega\right) \quad (2)$$

In this context, the photon frequency is denoted as $\hbar\omega$, the electronic charge as q, the volume of a unit cell as V, the polarization of the incident electric field as p, and the wave functions of electrons in the conduction band and valence band at a specific wave vector k are represented by ψ_k^c and ψ_k^v, respectively. By applying Kramers-Kronig relations, the real part of the dielectric function ($\varepsilon_1(\omega)$) can be derived from its imaginary part ($\varepsilon_2(\omega)$). Consequently, the complex refractive index ($N=n+ik$) and other optical properties can be computed by utilizing the complex dielectric function.

The absorption coefficient (α) is related to the extinction coefficient (k), speed of light in vacuum (c), and frequency (ω), as:

$$\alpha=\frac{2k\,\omega}{c} \quad (3)$$

2- 2- Thermodynamical and moisture stability

To examine the thermodynamic stability of 2D-perovskites, it is possible to calculate the formation energy (FE) using the following equation [12]:

$$FE=E(L_2BX_4)-2E(LX)-E(BX_2) \quad (4)$$

Here, E represents the total energy of the ground state for the respective components. The greater the absolute value of the FE, the more stable the material is considered to be.

The calculation of the adsorption energy of water on perovskites is performed as follows [13]:

$$E_{ads}=E_{(adsorbate/sub)}-\left[E_{adsorbate}+E_{sub}\right] \quad (5)$$

The adsorption energy (E_{ads}) is obtained by subtracting the sum of the total energies of the adsorbate (water molecules) and the isolated substrate system (perovskite surface) from the total energy of the adsorption system (water on the perovskite surface), as shown in Eq. (4). A negative value of E_{ads} indicates that the perovskite exhibits hydrophilicity, while a positive value indicates hydrophobicity.

3- Results and discussion

Table 1 presents the crystal data for $BA_2PbBr_{4-x}Cl_x$ (x=0, 2, and 4) at room temperature. The crystal structures of all these compounds demonstrate an orthorhombic phase, which is illustrated in Fig. 1 (a-c) [7].

Figure 2 illustrates the band structure and E_g of $BA_2PbBr_{4-x}Cl_x$ (x=0, 2, and 4). It is evident that the bandgap energy increases as the halide changes from Br (x=0) to a mixed halide (x=2) and then to Cl (x=4). The E_g values for BA_2PbBr_4, $BA_2PbBr_2Cl_2$, and BA_2PbCl_4 are 2.590 eV, 2.611 eV, and 3.070 eV, respectively. According to Table 2, our results for E_g are in good agreement with the other works.

All three materials exhibit a direct bandgap at the Γ point. In the Γ-Z region, the bands near the valence band maximum (VBM) and conduction band minimum (CBM) are flat, creating a barrier multiple quantum well structure. The flat band or non-dispersive part of the band structure in the reciprocal space corresponds to the out-of-plane direction (or

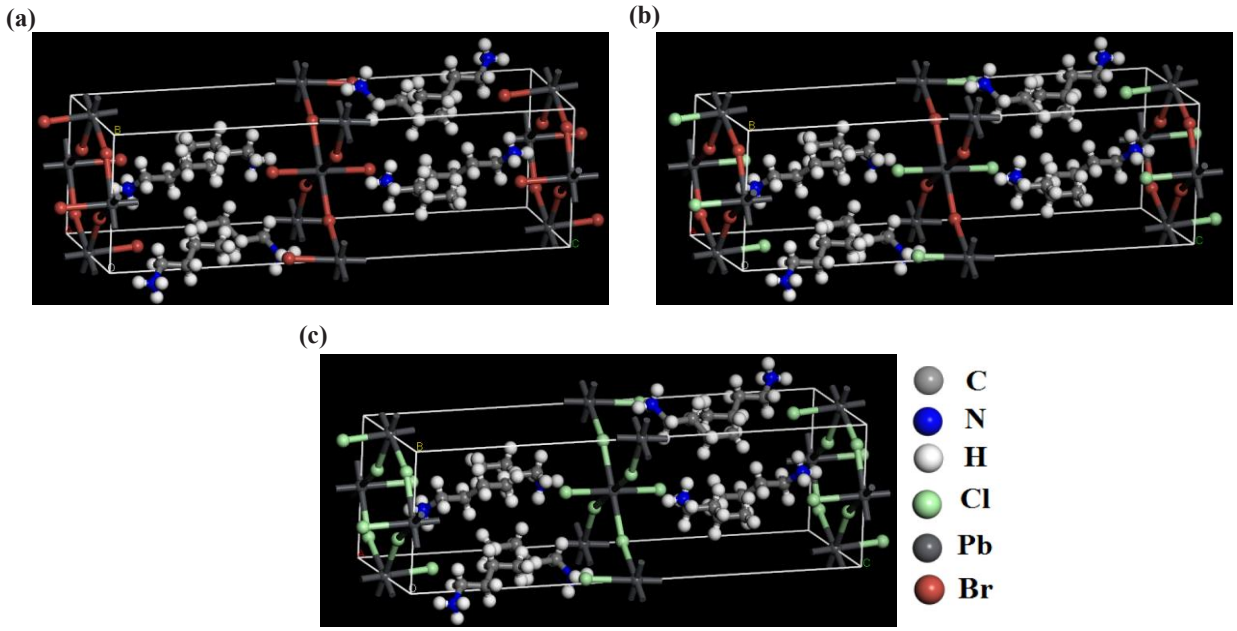

Fig. 1. Crystal structure of (a) BA_2PbBr_4, (b) $BA_2PbBr_2Cl_2$, and (c) BA_2PbCl_4

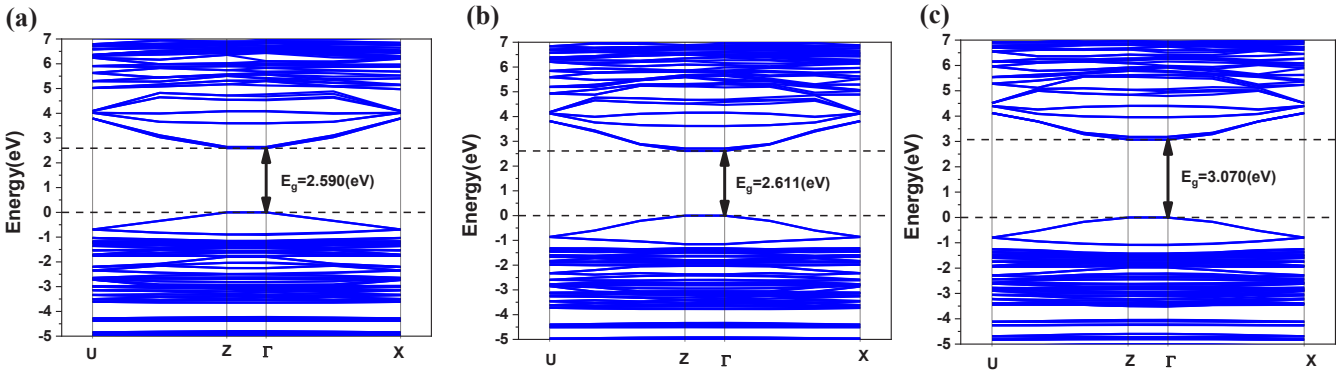

Fig. 2. Band structure for (a) BA_2PbBr_4, (b) $BA_2PbBr_2Cl_2$, and (c) BA_2PbCl_4

Table 2. The values bandgap for $BA_2PbBr_{4-x}Cl_x$ (x=0, 2, and 4)

Materials of 2D-perovskite	Eg (this work) with DFT calculation (eV)	Eg (other works) with DFT calculation (eV)
BA_2PbBr_4	2.590	2.63 [8], 2.50 [14]
$BA_2PbBr_2Cl_2$	2.611	*
BA_2PbCl_4	3.070	2.91 [14]

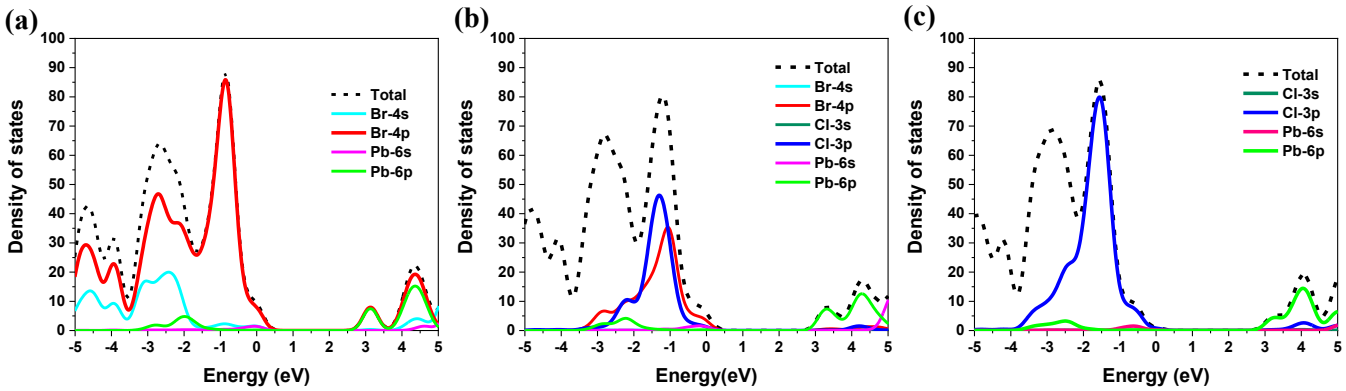

Fig. 3. PDOS curves for (a) BA_2PbBr_4, (b) $BA_2PbBr_2Cl_2$, and (c) BA_2PbCl_4

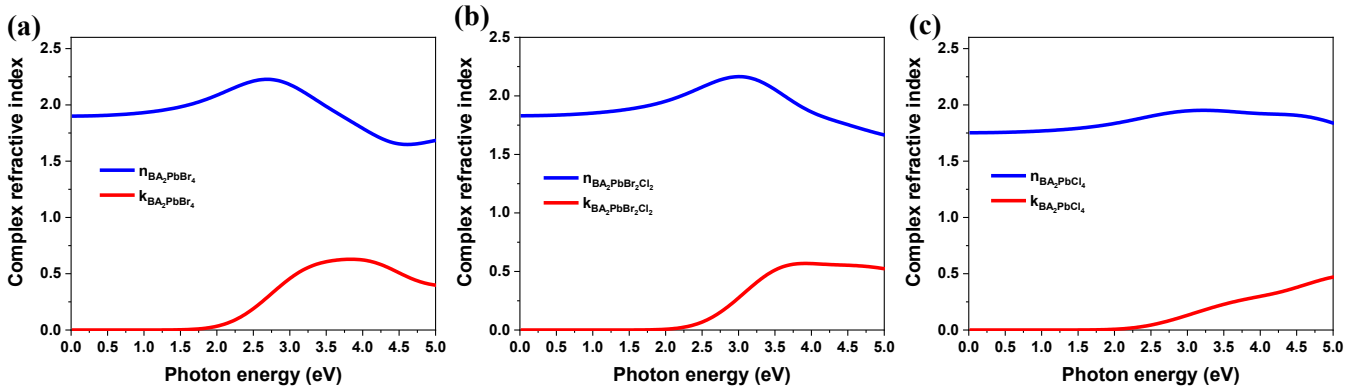

Fig. 4. Complex refractive index for (a) BA_2PbBr_4, (b) $BA_2PbBr_2Cl_2$, and (c) BA_2PbCl_4

the direction of the BA cation) in the direct space or equivalent to the quantum barrier. Consequently, the perovskites in the non-dispersive Γ-Z region have a large effective mass, and it causes non-transfer of carriers in the quantum barrier area and confinement of carriers in the well (i.e. inorganic layer) [8].

Fig. 3 displays the partial density of states (PDOS) for $BA_2PbBr_{4-x}Cl_x$ (x=0, 2, and 4). Observing these figures allows us to conclude that the VBM originates from an anti-bonding interaction between the s orbitals of Pb and the p orbitals of the halides (specifically, 6s-Pb with 4p-Br or 3p-Cl). On the other hand, the CBM arises from a weakly anti-bonding interaction between the 6p-Pb and the s orbitals of the halide. The interaction of orbitals in the edge bands creates a covalent bond (bonding, and anti-bonding) so that the VBM and the CBM are formed by covalent antibonding. In general, the VBM and CBM in 2D-perovskites are not directly affected by organic spacers, but these spacers can indirectly influence the band gaps by inducing structural distortion.

Figure 4 illustrates the variation of the complex refractive index for $BA_2PbBr_{4-x}Cl_x$ (x=0, 2, and 4) as a function of frequency. The results indicate that, unlike the E_g, the refractive index at zero frequency (n_0) decreases with the substitution of halides. Specifically, the value of n_0 changes from 1.90 for Br (x=0) to 1.830 for the mixed halide (x=2) and further decreases to 1.752 for Cl (x=4).

Figure 5 shows the absorption coefficient for $BA_2PbBr_{4-x}Cl_x$ (x=0, 2, and 4) as a function of photon energy. The first absorption peaks for BA_2PbBr_4, $BA_2PbBr_2Cl_2$, and BA_2PbCl_4 are 40419.504, 42275.362, and 43819.085 (cm^{-1}), respectively.

We utilize DFT to examine the effects of triaxial strains ranging from -3% to +3% on the bandgaps and refractive indices of the suggested perovskite materials. The outcomes depicted in Fig. 6 (a-c) display that the application of strain allows for the adjustment of the bandgaps and refractive indices of BA_2PbBr_4, $BA_2PbBr_2Cl_2$, and BA_2PbCl_4. This result illustrates the potential to control the bandgap of the

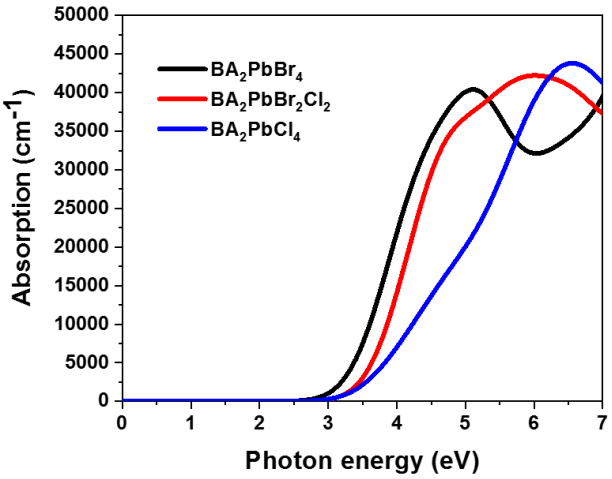

Fig. 5. The absorption spectra for BA2PbBr4-xClx (x=0, 2, and 4)

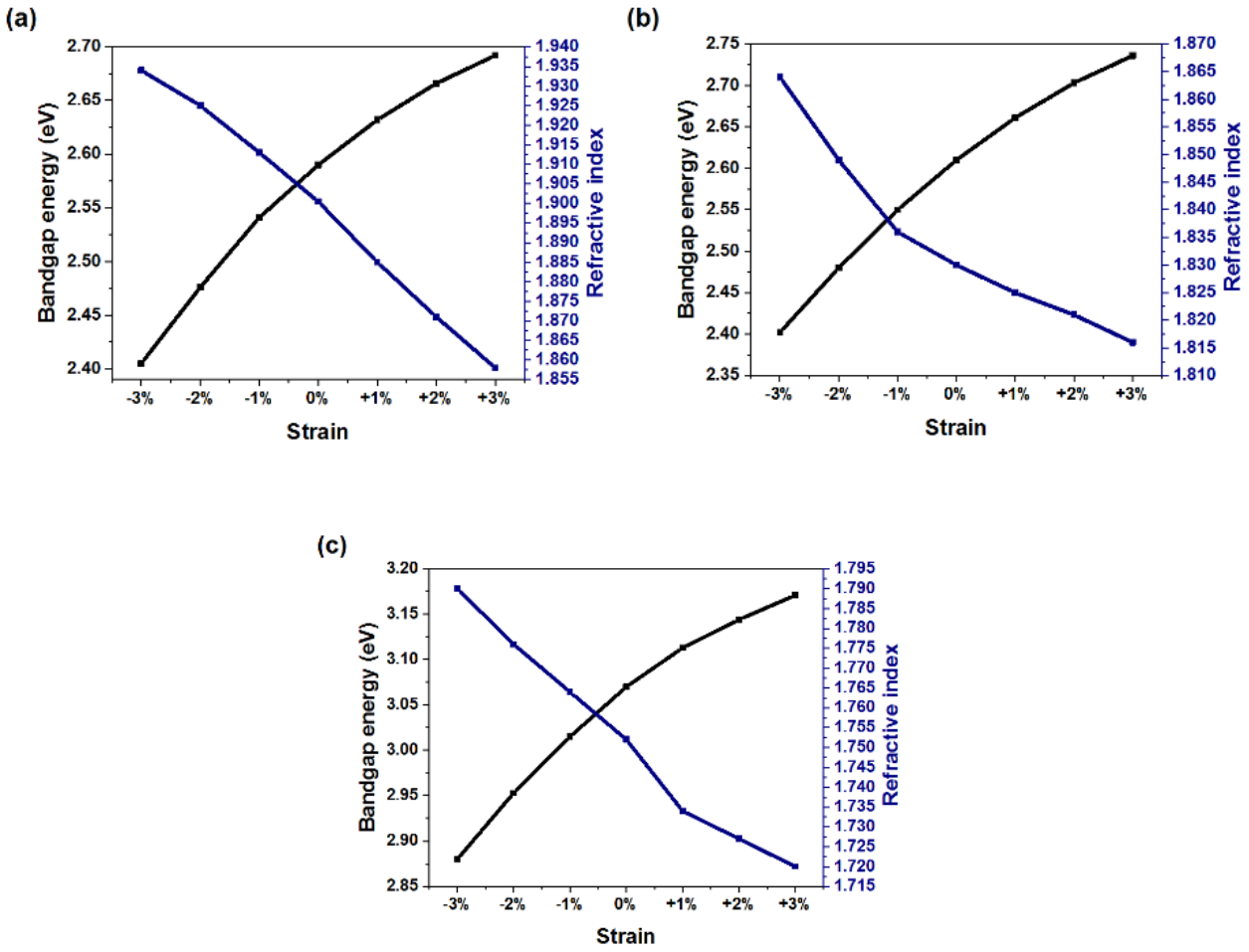

Fig. 6.Strain effect on bandgap energies and refractive indices of (a) BA_2PbBr_4, (b) $BA_2PbBr_2Cl_2$, and (c) BA_2PbCl_4

Table 3. Formation energy (FE) for the proposed 2D-perovskites

Materials of 2D-perovskite	$E(L_2PbX_4)$ (eV)	$E(PbX_2)$ (eV)	2*E(LX) (eV)	FE (eV)
BA_2PbBr_4	-10600.257	-4785.20	-5811.44	-3.88
$BA_2PbBr_2Cl_2$	-10771.207	-4785.608	-5981.49	-4.10
BA_2PbCl_4	-10942.509	-4956.052	-5982.26	-4.19

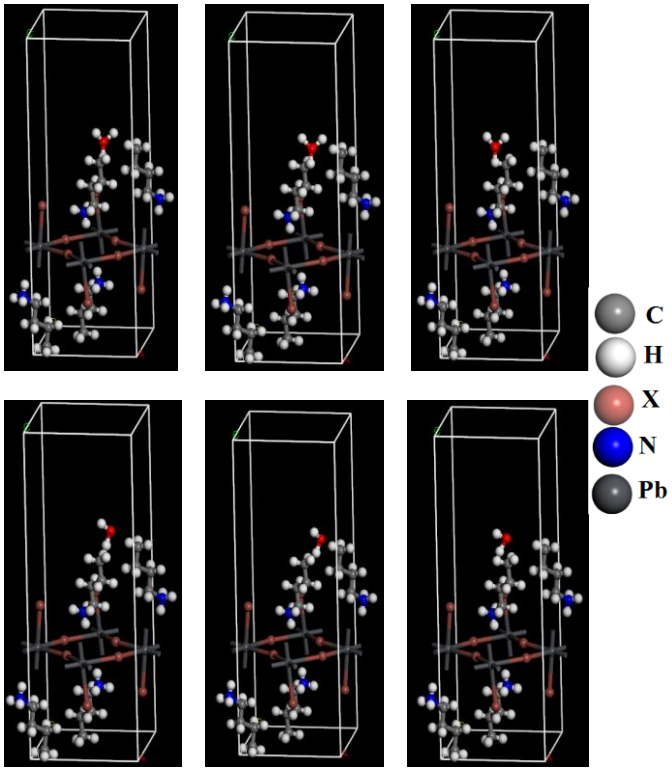

Fig. 7. H_2O on the surface of the suggested materials

proposed 2D-perovskite materials over a broad range through the use of strain.

Table 3 presents an examination of the thermodynamic stability of $BA_2PbBr_{4-x}Cl_x$ (x=0.2, and 4) by calculating the energy enthalpy of formation for the constituent components. The results reveal that $BA_2PbBr_2Cl_2$ exhibits intermediate thermodynamic stability when compared to BA_2PbBr_4 and BA_2PbCl_4. Additionally, BA_2PbBr_4 demonstrates a lower degree of thermodynamic stability in comparison to $BA_2PbBr_2Cl_2$ and BA_2PbCl_4, primarily due to its lower formation enthalpy energy.

In order to calculate E_{ads}, we examine six different scenarios for each material, as depicted in Fig. 7. It is important to mention that we only consider the perfect crystal structures for all the materials. The adsorption of water on the surfaces of perovskites is then evaluated in these six scenarios, and the resulting values are averaged and presented in Table 4. These materials exhibit excellent hydrophobic characteristics, with almost zero adsorption energy, indicating superior moisture stability compared to the majority of perovskites. Specifically, $BA_2PbBr_2Cl_2$ displays nearly a four-fold reduction in water molecule adsorption when compared to conventional 3D-perovskites [13]. Among the materials investigated, BA_2PbCl_4 demonstrates the highest level of stability, while BA_2PbBr_4 exhibits the lowest resistance to moisture.

We use ab initio molecular dynamic (AIMD) simulations to investigate how stable $BA_2PbBr_{4-x}Cl_x$ (x=0, 2, and 4) is when subjected to heat. The simulations are run for 10 picoseconds at a temperature of 298.15 K, with 10,000 simulation steps taken every 1 femtosecond. In Fig. 8 (a-c), we can see the

Table 4. Adsorption energy of water on BA_2PbBr_4-xClx (x=0, 2, and 4) surface

Materials of 2D-perovskite	$E_{water/perovskite}$ (eV)	$E_{perovskite}$ (eV)	E_{water} (eV)	E_{ads} (eV)
BA_2PbBr_4	-11068.764	-10599.769		-0.191
$BA_2PbBr_2Cl_2$	-11239.391	-10770.404	-468.804	-0.183
BA_2PbCl_4	-11410.351	-10941.368		-0.179

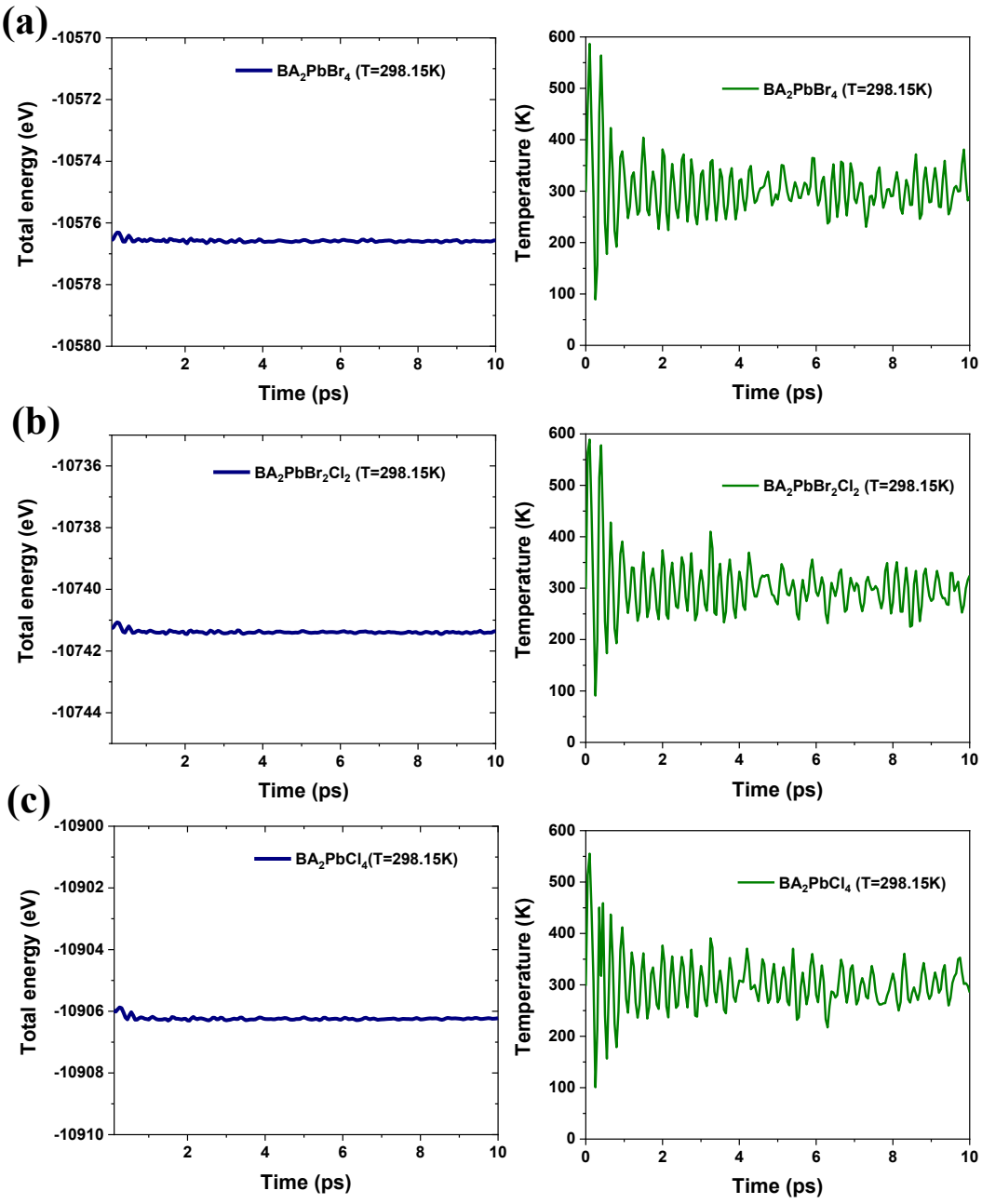

Fig. 8. AIMD simulations of the total energy and temperature for (a) BA_2PbBr_4, (b) $BA_2PbBr_2Cl_2$, and (c) BA_2PbCl_4

changes in the total energy and temperature versus time at 298.15 K. The energy shows a minimal fluctuation despite significant temperature variations. The variation of the total energies of the proposed materials is quite small within 0.2 eV, which is an order of magnetite smaller than the formation energies of these materials. Additionally, the chemical bonds and lattice parameters remained unchanged throughout the simulation, which suggests that the material is stable at room temperature.

These findings indicate that the mixed halide 2D-perovskite demonstrates favorable thermodynamic stability. Moreover, it possesses a direct bandgap and a low refractive index, rendering it a viable choice for implementation as an active layer in LED applications.

4- Conclusion

In summary, the electrical and optical properties of 2D-RP perovskites $BA_2PbBr_{4-x}Cl_x$ (x=0, 2, and 4) are investigated using DFT calculations. The results reveal that all three materials have a direct and tunable E_g. Increasing the amount of x in $BA_2PbBr_{4-x}Cl_x$ (x=0, 2, and 4) leads to a blue shift in E_g, and the value of the refractive index decreases. The PDOS plots indicate that the VBM is constructed by the antibonding interaction between the 6s-Pb and the 3p-Cl or 4p-Br orbitals, while the CBM dominates with 6p-Pb. All three materials are thermodynamically stable, as indicated by their negative formation energy. The AIMD method is utilized for studying the thermal stability of the proposed materials. The stability of these materials in relation to water is also investigated, aligning with the results of thermodynamic stability. Furthermore, the effects of strain on the bandgap and refractive index are also explored. In conclusion, $BA_2PbBr_{4-x}Cl_x$ (x=0, 2, and 4) is an appropriate option for the emissive layer in PeLEDs.

Acknowledgment

The authors would like to acknowledge the Iran National Foundation (INSF) support for this project.

References

[1] Veldhuis, S.A., Boix, P.P., Yantara, N., Li, M., Sum, T.C., Mathews, N. and Mhaisalkar, S.G., 2016. Perovskite materials for light-emitting diodes and lasers. Advanced Materials, 28(32), pp.6804-6834.

[2] Yin, W.J., Yang, J.H., Kang, J., Yan, Y. and Wei, S.H., 2015. Halide perovskite materials for solar cells: a theoretical review. Journal of Materials Chemistry A, 3(17), pp.8926-8942.

[3] Saadatmand, S.B., Shokouhi, S., Ahmadi, V. and Hamidi, S.M., 2023. Design and analysis of a flexible Ruddlesden–Popper 2D perovskite metastructure based on symmetry-protected THz-bound states in the continuum. Scientific Reports, 13(1), p.22411.

[4] Shokouhi, S., Saadatmand, S.B. and Ahmadi, V., 2023, October. First Principles Study of Optical and Electrical Properties for Mixed-halide 2D BA2PbBr4-xClx (x= 0, 2, and 4) as an Active Layer of Perovskite Light Emitting Diode. In 2023 5th Iranian International Conference on Microelectronics (IICM) (pp. 219-221). IEEE.

[5] Zhang, L., Sun, C., He, T., Jiang, Y., Wei, J., Huang, Y. and Yuan, M., 2021. High-performance quasi-2D perovskite light-emitting diodes: from materials to devices. Light: Science & Applications, 10(1), p.61.

[6] Xing, J., Zhao, Y., Askerka, M., Quan, L.N., Gong, X., Zhao, W., Zhao, J., Tan, H., Long, G., Gao, L. and Yang, Z., 2018. Color-stable highly luminescent sky-blue perovskite light-emitting diodes. Nature Communications, 9(1), p.3541.

[7] Zhou, G., Li, M., Zhao, J., Molokeev, M.S. and Xia, Z., 2019. Single-Component White-Light Emission in 2D Hybrid Perovskites with Hybridized Halogen Atoms. Advanced Optical Materials, 7(24), p.1901335.

[8] Silver, S., Yin, J., Li, H., Brédas, J.L. and Kahn, A., 2018. Characterization of the valence and conduction band levels of n= 1 2D perovskites: a combined experimental and theoretical investigation. Advanced Energy Materials, 8(16), p.1703468.

[9] Ma, L., Dai, J. and Zeng, X.C., 2017. Two-Dimensional Single-Layer Organic-Inorganic Hybrid Perovskite Semiconductors. Advanced Energy Materials, 7(7), p.1601731.

[10] Segall, M.D., Lindan, P.J., Probert, M.A., Pickard, C.J., Hasnip, P.J., Clark, S.J. and Payne, M.C., 2002. First-principles simulation: ideas, illustrations, and the CASTEP code. Journal of Physics: Condensed Matter, 14(11), p.2717.

[11] Palik, E.D. ed., 1998. Handbook of Optical Constants of Solids (Vol. 3). Academic Press.

[12] Yang, Y., Gao, F., Gao, S. and Wei, S.H., 2018. Origin of the stability of two-dimensional perovskites: a first-principles study. Journal of Materials Chemistry A, 6(30), pp.14949-14955.

[13] Hu, J., Ma, X., Duan, W., Liu, Z., Liu, T., Lv, H., Huang, C., Miao, L. and Jiang, J., 2020. First-Principles Calculations of Graphene-Coated CH3NH3PbI3 toward Stable Perovskite Solar Cells in Humid Environments. ACS Applied Nano Materials, 3(8), pp.7704-7712.

[14] Varghese, A., Yin, Y., Wang, M., Lodha, S. and Medhekar, N.V., 2022. Near-Infrared and Visible-Range Optoelectronics in 2D Hybrid Perovskite/Transition Metal Dichalcogenide Heterostructures. Advanced Materials Interfaces, 9(14), p.2102174.

HOW TO CITE THIS ARTICLE

S. Shokouhi, S. B. Saadatmand, V. Ahmadi, F. Arabpour Roghabadi. Comprehensive Study on Optical, Electrical, and Stability Properties of BA2PbBr4-xClx (x = 0, 2, and 4) Ruddlesden Popper Perovskites for High-Performance PeLEDs. AUT J Electr Eng, 56(3) (2024) 389-398.

DOI: 10.22060/eej.2024.22949.5577